Title

External Factors Modulating Vaping-Induced Thermal Degradation of Vitamin E Acetate

Journal

Chemical Research in Toxicology, 36(1)

ISSN

0893-228X

Authors

Canchola, Alexa
Langmo, Siri
Meletz, Ruth
et al.

Publication Date

2023-01-16

DOI

10.1021/acs.chemrestox.2c00298

Peer reviewed

Chemical Research in Toxicology

pubs.acs.org/crt

Article

External Factors Modulating Vaping-Induced Thermal Degradation of Vitamin E Acetate

Published as part of the Chemical Research in Toxicology virtual special issue "Tobacco: Chemistry, Mechanisms, Biomarkers and Disease Prevention".

Alexa Canchola, Siri Langmo, Ruth Meletz, Michael Lum, and Ying-Hsuan Lin*

Cite This: *Chem. Res. Toxicol.* 2023, 36, 83−93

Read Online

ACCESS | Metrics & More | Article Recommendations | Supporting Information

ABSTRACT: Despite previous studies indicating the thermal stability of vitamin E acetate (VEA) at low temperatures, VEA has been shown to readily decompose into various degradation products such as alkenes, long-chain alcohols, and carbonyls such as duroquinone (DQ) at vaping temperatures of <200 °C. While most models simulate the thermal decomposition of e-liquids under pyrolysis conditions, numerous factors, including vaping behavior, device construction, and the surrounding environment, may impact the thermal degradation process. In this study, we investigated the role of the presence of molecular oxygen (O_2) and transition metals in promoting thermal oxidation of e-liquids, resulting in greater degradation than predicted by pure pyrolysis. Thermal degradation of VEA was performed in inert (N_2) and oxidizing atmospheres (clean air) in the absence and presence of Ni−Cr and Cu−Ni alloy nanopowders, metals commonly found in the heating coil and body of e-cigarettes. VEA degradation was analyzed using thermogravimetric analysis (TGA) and gas chromatography/mass spectrometry (GC/MS). While the presence of O_2 was found to significantly enhance the degradation of VEA at both high (356 °C) and low (176 °C) temperatures, the addition of Cu−Ni to oxidizing atmospheres was found to greatly enhance VEA degradation, resulting in the formation of numerous degradation products previously identified in VEA vaping emissions. O_2 and Cu−Ni nanopowder together were also found to significantly increase the production of OH radicals, which has implications for e-liquid degradation pathways as well as the potential risk of oxidative damage to biological systems in real-world vaping scenarios. Ultimately, the results presented in this study highlight the importance of oxidation pathways in VEA thermal degradation and may aid in the prediction of thermal degradation products from e-liquids.

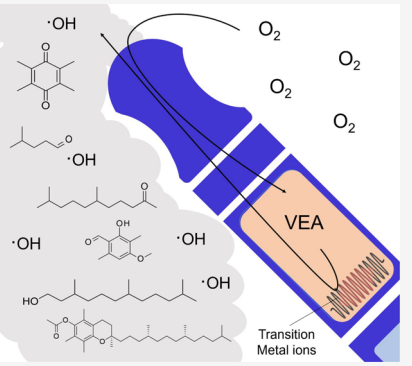

1. INTRODUCTION

Recent research has revealed that the inhalation of aerosols released by e-cigarettes has the potential to negatively impact the lungs of users, despite the prevalent assumption of safety among e-cigarette consumers.[1,2] Though many commonly used e-liquid ingredients, including propylene glycol (PG), glycerin (VG), and various flavoring agents, are considered safe for consumption or dermal absorption, emitted aerosols are complex mixtures of compounds formed from the thermal degradation of e-liquids that occurs during the vaping process.[3] This process results in the formation of emission products with different physiochemical properties and a risk of toxicity potentially greater than that posed by the parent e-liquids.[3−6] For example, vitamin E acetate (VEA), the proposed cause of the e-cigarette or vaping-associated lung injury (EVALI) outbreak in the United States in 2019, has been found to decompose into thermal degradation products, including vitamin E (VE), various long-chain alcohols, alkenes, carbonyls, and, most notably, the reactive species duroquinone (DQ) and ketene.[3,4,7−9] While VEA itself is perceived as safe, the inhalation of electrophilic species like DQ produced during vaping poses a serious risk of oxidative damage to lung tissue.[4,9−11] As such, to understand the potential health risk to users, the prediction of the thermal degradation behavior of various e-liquids through computational and experimental methods has been of particular interest in recent e-cigarette research.

In addition to potentially toxic organic products, there is also the potential for the release of metals into the e-liquid and e-cigarette emissions at potentially toxic concentrations. e-Cigarette devices often contain various transition metals, including Ni, Fe, Cu, Cr, etc.[12−15] A recent study by Williams et al.[16] detected particles containing metals such as Sn, Ag, Fe,

Received: September 23, 2022
Published: December 19, 2022

Ni, Al, and Cr in e-cigarette aerosol emissions. In a similar study, McDaniel et al.[12] found various levels of transition metals, including Cr, Cu, and Ni, in e-cigarette aerosols and leached into the e-liquid. These metals pose a risk of metal toxicity to vape users upon inhalation,[17] and recent studies have suggested a potential catalytic role in the thermal degradation of e-liquids, particularly at low temperatures.[7,18,19]

There are several driving factors that have been suggested to influence the physiochemical properties of e-cigarette emissions, including puffing topography[20,21] and temperature.[7,22] Changes in the temperature used to heat e-liquids during vaping have been demonstrated to affect the size and volume distribution of emitted aerosols,[21,23] the release of metals[24] or reactive oxygen species (ROS),[25−27] and the chemical composition of e-cigarette emissions.[22,28] Though use of VEA is not widespread in commercial e-liquids, the extensive efforts to characterize vaping emission products of VEA allow it to be more easily used as a model compound to monitor changes caused by various vaping parameters. In ref 7, our lab found a temperature dependence in the chemical composition of VEA vaping emissions when VEA was vaped at temperatures ranging from 176 to 356 °C and demonstrated discrepancies in chemical composition when VEA was vaped versus heated without the device. While previous theoretical and experimental studies have demonstrated VEA to be thermally stable up to 250 °C under pure pyrolysis conditions,[29] our studies indicate that VEA degrades into compounds such as DQ when vaped at temperatures of <200 °C. Under pure pyrolysis conditions in an inert argon atmosphere, VEA did not appear to degrade until the temperature exceeded 300 °C. Furthermore, previous studies in our lab have frequently detected DQ in vaping emissions at temperatures significantly lower than those predicted by theoretical calculations.[3,4,7]

Discrepancies in the product distribution of VEA vaping emissions and pyrolysis-simulated VEA breakdown at equitable temperatures may indicate the influence of external factors, such as the presence of atmospheric oxygen molecules (O_2) and metal catalysts, on e-liquid degradation. In e-cigarette systems, the presence of metal filament wires has been suggested to have strong catalytic effects on the thermal degradation of PG and VG, reducing the temperature needed to observe carbonyl-containing compounds in vaping emissions.[18,19] Furthermore, metal catalysis has been found to be an important factor in thermal degradation pathways in analyses of systems such as biochar.[30] The presence of O_2 has also been found to greatly decrease the temperature required to observe the thermal degradation of PG and VG and may play an important role in the low-temperature degradation of e-liquids.[7,31,32]

For this reason, we hypothesized that the presence of O_2 and transition metals in the e-cigarette body promotes the thermal oxidation of e-liquids, resulting in greater degradation at low temperatures than what is predicted by pure pyrolysis. To address this hypothesis, we used VEA as a model compound to compare how thermal degradation of organics may be altered when they are heated under inert (N_2) and oxidizing (clean air) atmospheres, with and without the addition of metal alloys. To monitor these changes, we used a combination of gas chromatography/mass spectrometry (GC/MS) and thermogravimetric analysis (TGA). Direct measurement of hydroxyl (OH) radicals was also carried out using the fluorometric terephthalate (TPT) assay. The results of this study further our understanding of the influence of O_2 and metals on the thermal degradation of organic compounds and the resulting health risks upon inhalation.

2. MATERIALS AND METHODS

2.1. Materials. Vitamin E acetate (DL-α-tocopherol acetate, VEA, >97%) and disodium terephthalate (TPT, >99%) were purchased from Tokyo Chemical Industry (TCI America, Inc.). Nickel−chromium (Ni−Cr, 99.9%, 8:2 Ni:Cr) and copper−nickel (Cu−Ni, 99.9%, 5:5 Cu:Ni) alloy nanopowders were purchased from US Research Nanomaterials Inc. 1,2,3-Trichlorobenzene (1,2,3-TCB, 98%) and 2-hydroxyterephthalic acid (2-OHTA, >98%) were purchased from Alfa Aesar. Acetonitrile (ACN, 99.95%) was purchased from Fisher Chemical. Phosphate-buffered saline (PBS, 1×) was purchased from Corning.

2.2. Thermogravimetric Analysis (TGA). TGA was performed on a Netzsch TG 209 F1 Libra instrument to characterize the mass changes (loss or gain) of VEA as a function of temperature in the inert and oxidizing atmospheres due to volatilization, decomposition, or oxidation. VEA was added to a 6.8 nm diameter alumina crucible using a rubber syringe with enough sample to coat the bottom of the crucible in a thin layer, which gave a sample mass of approximately 10 mg. The exact mass of the crucible and sample was measured by the instrument at the start of each experiment. VEA was heated using a temperature ramp of 10 K min^{-1} using either N_2 or clean air as a carrier gas. The instrument was operated using a flow rate of 40 mL min^{-1} and an instrument protective flow rate of 10 mL min^{-1}.

2.3. Pyrolysis GC/MS. Pyrolysis gas chromatography/mass spectrometry (Pyr-GC/MS) was used to analyze the pyrolysis products of VEA. A CDS 5150 Pyroprobe (CDC Analytical, Inc.) was used to heat 250 mg of VEA at 356 °C in either N_2 or clean air environments. The pyrolysis products were directly injected onto an Agilent HP5-MS fused silica column and analyzed using GC/MS [Agilent 7890 GC and 5975 inert MSD equipped with an electron ionization (EI) ion source] following the ASTM D3452-06 standard method.[33]

2.4. Tube Furnace Experiments. Thermal degradation of VEA was simulated using a tube furnace reactor system (OTF-1200X, MTI Corp.) as described in our previous work.[7] One hundred milligrams of VEA was weighed into an alumina crucible, and the crucible placed in a high-temperature quartz tube furnace. Either ultra-high-purity N_2 (Airgas Inc.) or Ultra Zero grade clean air (Airgas Inc.) was used as a carrier gas at a flow rate of 0.18 L min^{-1} to deliver off-gassing products from VEA volatilization or thermal degradation to a cold trap apparatus. The cold trap was kept on dry ice to allow the collection of condensed emission products. The temperature was initially set to 30 °C, ramped to either 356 or 176 °C at a rate of 10 °C min^{-1}, and held for 1 min. The crucible was reweighed after each experiment to determine the mass loss, and 1 mL of ACN was added to the cold trap to dissolve captured emission products for chemical analysis. Cold trap samples were concentrated to 150 μL under a gentle N_2 gas stream. A 50 μL aliquot of each sample was taken for chemical analysis; 5 μL a 1,2,5-TCB (2 μg $μL^{-1}$) solution was added to each sample as an internal standard.

VEA was heated in N_2 and clean air environments in the absence and presence of 10 mg of Ni−Cr or Cu−Ni alloy nanopowders, which were chosen as representative components of e-cigarette heating coils.[12] A total of six experiments were performed, each with three replicates for statistical analysis.

2.5. GC/MS Analysis of Tube Furnace Samples. The samples collected from the tube furnace experiments were analyzed using GC/MS (Agilent 6890N GC and 5975C inert MSD equipped with an EI ion source). Helium was used as the carrier gas. To quantify more polar oxygenated products such as DQ in the collected emissions, 2 μL of each sample was directly injected onto a Restek Rtx-VMS fused silica column [30 m × 0.25 mm i.d. (inside diameter), 1.4 μm film]. The temperature of the GC started at 35 °C, was held for 1 min, was ramped to 240 °C at a rate of 10 °C min^{-1}, and was held for 4 min. To quantify nonpolar compounds such as VEA and 1-pristene, 1 μL

https://doi.org/10.1021/acs.chemrestox.2c00298
Chem. Res. Toxicol. 2023, 36, 83−93

of each sample was injected onto an Agilent J&W DB-5MS column (30 m × 0.25 mm i.d., 0.25 μm film). The temperature started at 60 °C, was held for 1 min, was ramped to 310 °C at a rate of 10 °C min^{-1}, and was held for 5 min.

2.6. Generation of OH Radicals. Generation of OH radicals was measured using the fluorescent probe disodium terephthalate (TPT), which readily reacts with OH radicals to form the stable fluorescent product 2-OHTA.[34−36] As the formation rate of 2-OHTA is directly proportional to the generation of OH radicals (1:1), the fluorescence of 2-OHTA can be measured using a microplate reader and used to directly quantify OH radical formation during VEA thermal degradation. The outflow of the tube furnace was bubbled through a 30 mL mini-impinger filled with 15 mL of a 5 mM TPT solution in 1× PBS. Once heating was finished, 100 μL of the solution was immediately transferred to a black, clear-bottom 96-well plate (Corning). Fluorescence was measured using a TECAN Spectrafluor plus microplate reader (excitation at 310 nm, emission at 422 nm). The concentration of 2-OHTA produced was determined on the basis of a calibration curve of 2-OHTA standard fluorescence in 1× PBS (Figure S1).

3. RESULTS AND DISCUSSION

3.1. TGA. Dynamic TGA was used to continuously measure the change in the mass of VEA as the temperature was increased to determine the loss of gaseous byproducts formed during pure VEA pyrolysis under N_2 and clean air atmospheres. The results of TGA of VEA heated under N_2 and clean air carrier gases are shown in Figure 1. A summary of

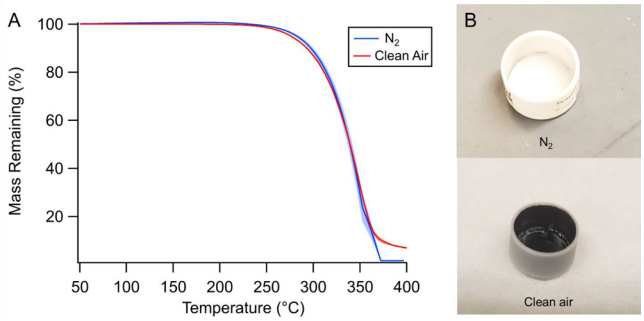

Figure 1. (A) TGA curve of VEA heated in N_2 and clean air atmospheres. Results are expressed as the mean of three replicates (n = 3) ± the standard error of the mean (SEM; represented by the shaded area surrounding each line). (B) Images of crucibles after they had been heated to 400 °C; 1.61% of initial mass remained in the crucible heated in N2 (top), and 6.94% remained in the crucible heated in clean air (bottom).

the major differences in the percent mass loss of VEA at various temperatures can be found in Table S1. Ultimately, the percent mass of VEA remaining is consistently greater in the oxidizing atmosphere than in the inert atmosphere. Volatilization of VEA appeared to begin around 250 °C in the inert atmosphere, which agrees with previous literature regarding the boiling point and pyrolysis of VEA.[29,37] Clean air, in comparison, did not show signs of volatilization until temperatures of ≥300 °C had been reached, demonstrating a substantially slower rate of degradation than when heated in N_2 (Figure 1A). By 400 °C, 1.61% of VEA remained in the crucible in the inert atmosphere, compared to 6.94% that remained in the clean air atmosphere. Furthermore, crucibles heated in N_2 contained either no residue or small amounts of VEA oil remaining inside after heating; in contrast, crucibles heated in clean air contained visible black residue, likely from the mineralization of VEA in the presence of clean air (Figure 1B). It is likely that, in clean air, VEA may be oxidized by O_2 to form various oxidation products that require greater temperatures to undergo the transition to the gas phase or decompose into further volatile degradation products. Residue permanently remaining from VEA mineralization may also explain why complete consumption of VEA by 400 °C cannot be seen in clean air compared to the N_2 atmosphere. Notably, the presence of O_2 alone did not appear to promote VEA phase transfer at low temperatures but did result in the production of degradation products with chemical properties different from those of VEA alone.

3.2. Pyr-GC/MS. To further investigate the influence of O_2 on the chemical composition of VEA thermal degradation products, Pyr-GC/MS was used to monitor the breakdown of VEA at 356 °C in N_2 and clean air. This temperature was chosen because 356 °C was the highest average coil temperature to which VEA was exposed while vaping with a CCell TH2 cartridge in our previous work.[7] At this temperature, substantial degradation could be observed in the analysis of vaping emissions, but simulation of pure pyrolysis with inert argon as a carrier gas showed a significantly decreased number and concentration of degradation products.

The total ion chromatograms (TICs) obtained from Pyr-GC/MS in each atmosphere are shown in Figure 2. A targeted search was performed for previously reported VEA vaping emission products using the NIST 2008 spectral database. A match score of ≥850 and a probability of ≥50% were considered a good match; authentic standards were used to confirm identified peaks when commercially available. Though VEA shows substantial degradation into various compounds in vaping scenarios at 356 °C,[7] no substantial degradation could be observed after heating in the inert N_2 atmosphere (Figure 2A). Major peaks for VE and VEA were visible at retention times of 38 min (peak 2) and 40.3 min (peak 3), respectively, indicating volatilization of VEA and potential loss of the acetate group at 356 °C. The dominant peaks of VE and VEA are assumed to correspond to the α-isomers based on the initial standard used; smaller peaks corresponding to other common isomers (β, γ, and δ) can also be seen but cannot be differentiated due to the resolution of the mass spectrometer used. Finally, a peak corresponding to the N_2 carrier gas can be seen at 3.7 min (peak 1). Four peaks in this spectrum could not be identified due to a lack of NIST matches.

When VEA and VE were heated to the same temperature in clean air, their concentrations decreased below the detection limit of the instrument and could not be observed. Instead, a wide range of degradation products commonly observed in vaping emissions could be seen in the resulting TIC (Figure 2B). Ultimately, analysis of these results found the presence of 4-methyl-1-pentanal (peak 1; t_R = 9.805 min), 4-methyl-1-decene (peak 2; t_R = 15.830 min), 3,7,11-trimethyl-1-dodecanol (peak 3; t_R = 26.84 min), durohydroquinone (DHQ) (peak 4; t_R = 27.103 min), 1-pristene (peak 5; t_R = 28.073 min), and 2-hydroxy-4-methoxy-3,6-dimethyl benzaldehyde (peak 6; t_R = 28.834 min), all of which have been previously detected in VEA vaping emissions.[4,7−10,38,39] DQ was not observed at levels above the detection limit of the instrument, though DQ formation can be assumed due to the detection of 1-pristene and DHQ.[9,39] Ultimately, it is clear that the presence of O_2 when VEA is heated results in the production of compounds often found in VEA vaping emissions, indicating the importance of oxidation pathways during vaping thermal degradation.

https://doi.org/10.1021/acs.chemrestox.2c00298
Chem. Res. Toxicol. 2023, 36, 83−93

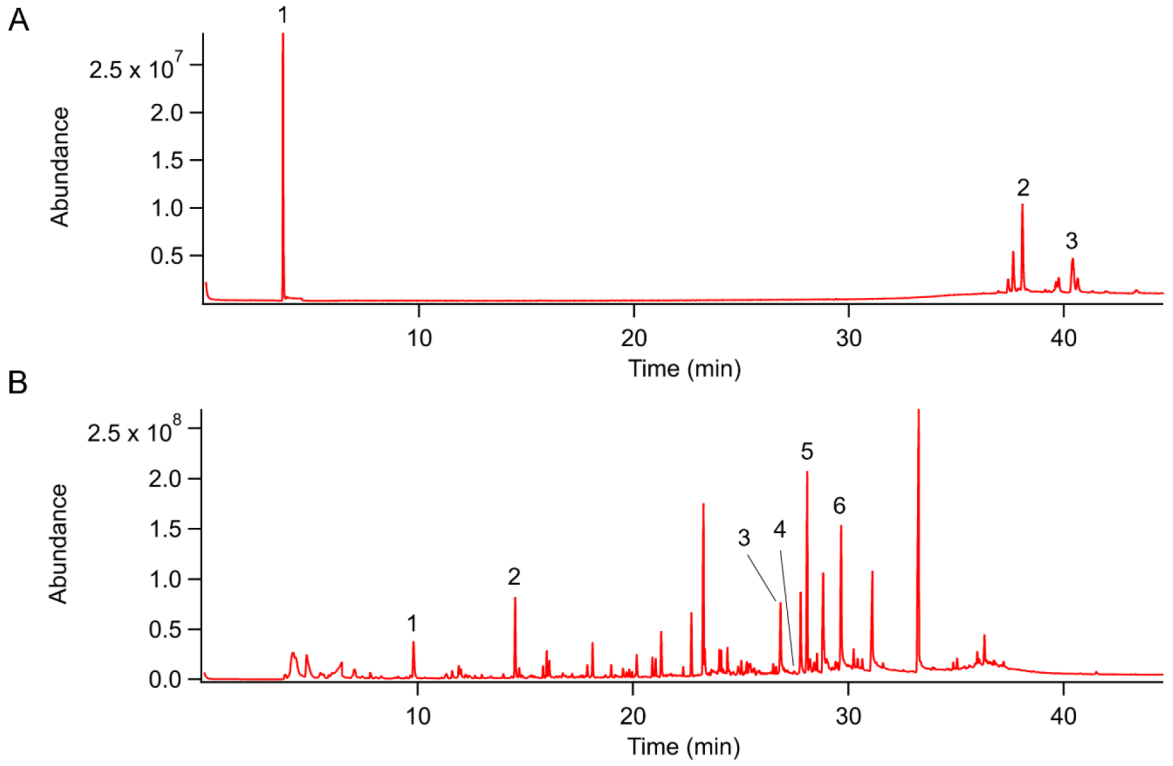

Figure 2. Total ion chromatograms (TICs) obtained from Pyr-GC/MS of VEA in (A) N_2 and (B) clean air atmospheres.

3.3. GC/MS Analysis of VEA Thermal Degradation. VEA was then heated in a tube furnace reactor under six different environmental conditions to investigate the effect of the presence of O_2 and metal alloys on the chemical composition of VEA thermal degradation products at high (356 °C) and low (176 °C) temperatures. The amount of mass consumed (i.e., lost as gas-phase compounds through volatilization, decomposition, or oxidation) during the tube furnace reaction at 356 °C remained mostly constant between the environmental conditions, though VEA heated with Cu−Ni alloy nanopowder showed a slight increase in mass consumption compared to the others. The greatest average mass consumption was seen in VEA heated in clean air with Cu−Ni nanopowder (Figure S2A).

3.3.1. High-Temperature Experiments at 356 °C. Off-gassing products were collected using a cold trap apparatus and analyzed using GC/MS. The TICs obtained from heating VEA under each condition at 356 °C are shown in Figure 3. Similar to the results obtained in our prior study,[7] substantial VEA degradation was not observed under inert N_2 atmospheres, nor did the addition of metal nanopowders significantly alter the resulting product distribution. In contrast, the number and abundance of VEA degradation products substantially increased when VEA was heated in oxidizing atmospheres. Furthermore, VEA heated in an oxidizing atmosphere in the presence of Cu−Ni demonstrated the greatest number of peaks compared to other environments, indicating greater degradation of VEA. In addition, after heating in N_2 environments (regardless of the addition of metal nanopowders), VEA oil remained clear with no visible discoloration, whereas after heating in O_2, VEA oil became a dark orange-brown color, indicating the formation of various thermal degradation products in oxidizing atmospheres (Figure S3).

Six representative degradation products were then chosen for quantification to further investigate how O_2 and metal alloys influence the identity and concentration of compounds formed from VEA degradation. These compounds include VEA [t_R = 27.32 min (Figure 3A,C)], 1-pristene [t_R = 19.89 min (Figure 3B,D)], DQ [t_R = 16.69 min (Figure 3B,D)], 2-hydroxy-4-methoxy-3,6-dimethyl benzaldehyde [t_R = 22.67 min (Figure 3B,D)], 3,7,11-trimethyl-1-dodecanol [t_R = 19.21 min (Figure 3B,D)], and 6,10-dimethyl-2-undecanone [t_R = 17.24 min (Figure 3B,D)]. To quantify the production of each compound, the peak areas were normalized to that of the 1,2,3-TCB internal standard. The concentration of each compound was then expressed as the mass of product normalized to the initial mass of VEA (i.e., milligrams of product recovered per milligram of initial VEA). A two-way analysis of variance (ANOVA) with either a Tukey HSD or Šidák posthoc analysis was used to determine the statistical significance of treatments. The masses of the representative thermal degradation products formed at 356 °C are shown in Figure 3E.

Regardless of metal alloys, a significantly greater mass of VEA was found in VEA emissions generated under N_2 than under clean air, indicating greater decomposition of VEA in the presence of O_2 than in inert atmospheres. For 1-pristene, the addition of Ni−Cr or Cu−Ni alloy nanopowder in the inert environment resulted in significantly greater mass compared to the absence of metals, with Cu−Ni resulting in the greatest mass across all environments. There was no statistical difference between clean air environments. 3,7,11-Trimethyl-1-dodecanol consistently showed a slightly larger (though not statistically significant) masses in the inert atmosphere than in the oxidizing atmosphere. Interestingly, for DQ, 2-hydroxy-4-methoxy-3,6-dimethyl benzaldehyde, and 6,10-dimethyl-2-undecanone, we observed significant differences in recovered masses between the inert and oxidizing atmospheres in the

https://doi.org/10.1021/acs.chemrestox.2c00298
Chem. Res. Toxicol. 2023, 36, 83−93

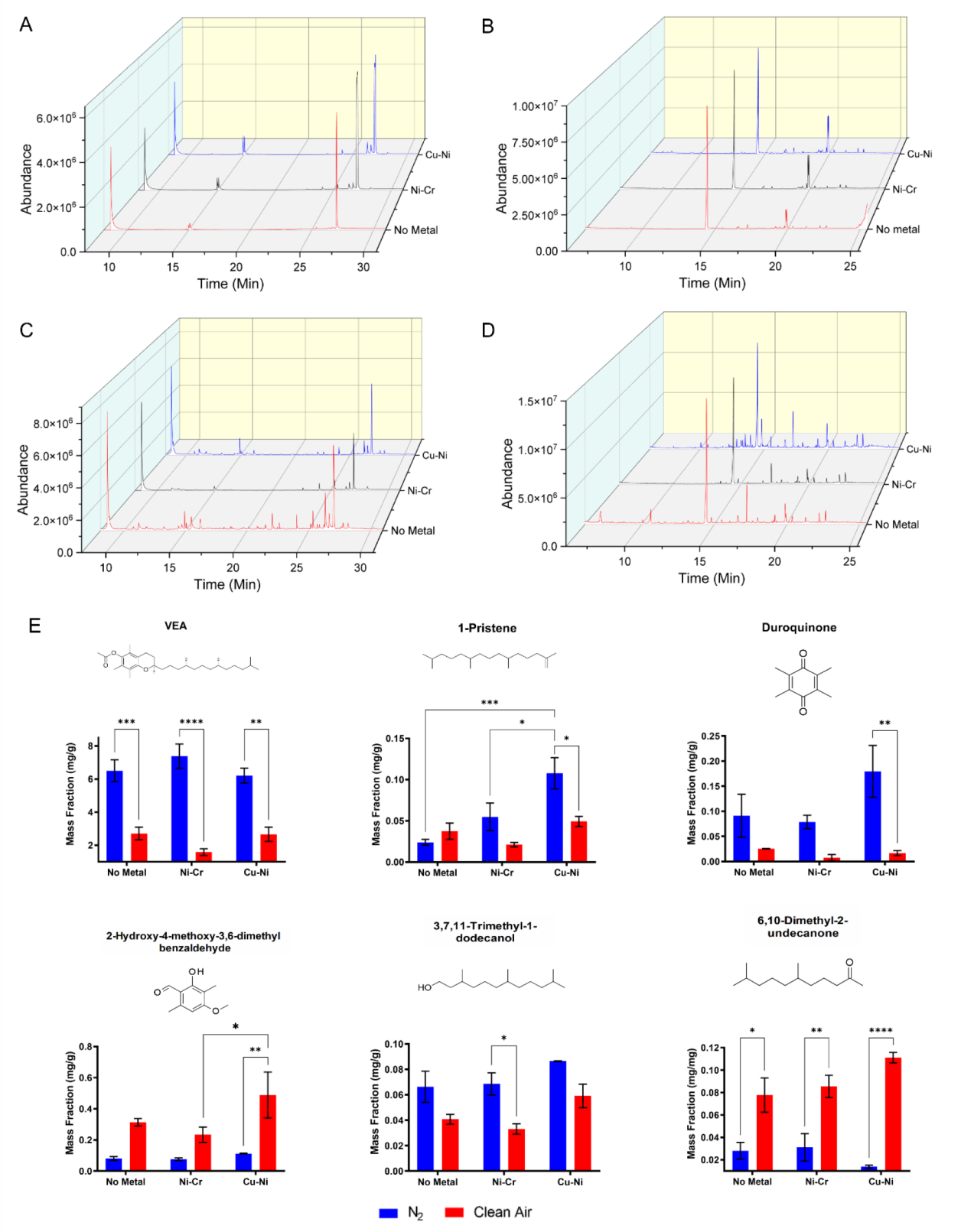

Figure 3. VEA product distribution under six different environmental conditions at 356 °C. Total ion chromatograms (TICs) were obtained from VEA pyrolysis in (A) N_2 environments in a nonpolar separation column, (B) N_2 in a polar separation column, (C) clean air in a nonpolar separation column, and (D) clean air in a polar separation column. (E) Masses of thermal degradation products, including VEA, 1-pristene, duroquinone, 2-hydroxy-4-methoxy-3,6-dimethyl benzaldehyde, 3,7,11-trimethyl-1-dodecanol, and 6,10-dimethyl-2-undecanone, formed under N_2 and clean air atmospheres at 356 °C. Results are expressed as means ± SEM (n = 3). An asterisk indicates $p < 0.05$. Two asterisks indicate $p < 0.01$. Three asterisks indicate $p < 0.001$.

https://doi.org/10.1021/acs.chemrestox.2c00298
Chem. Res. Toxicol. 2023, 36, 83−93

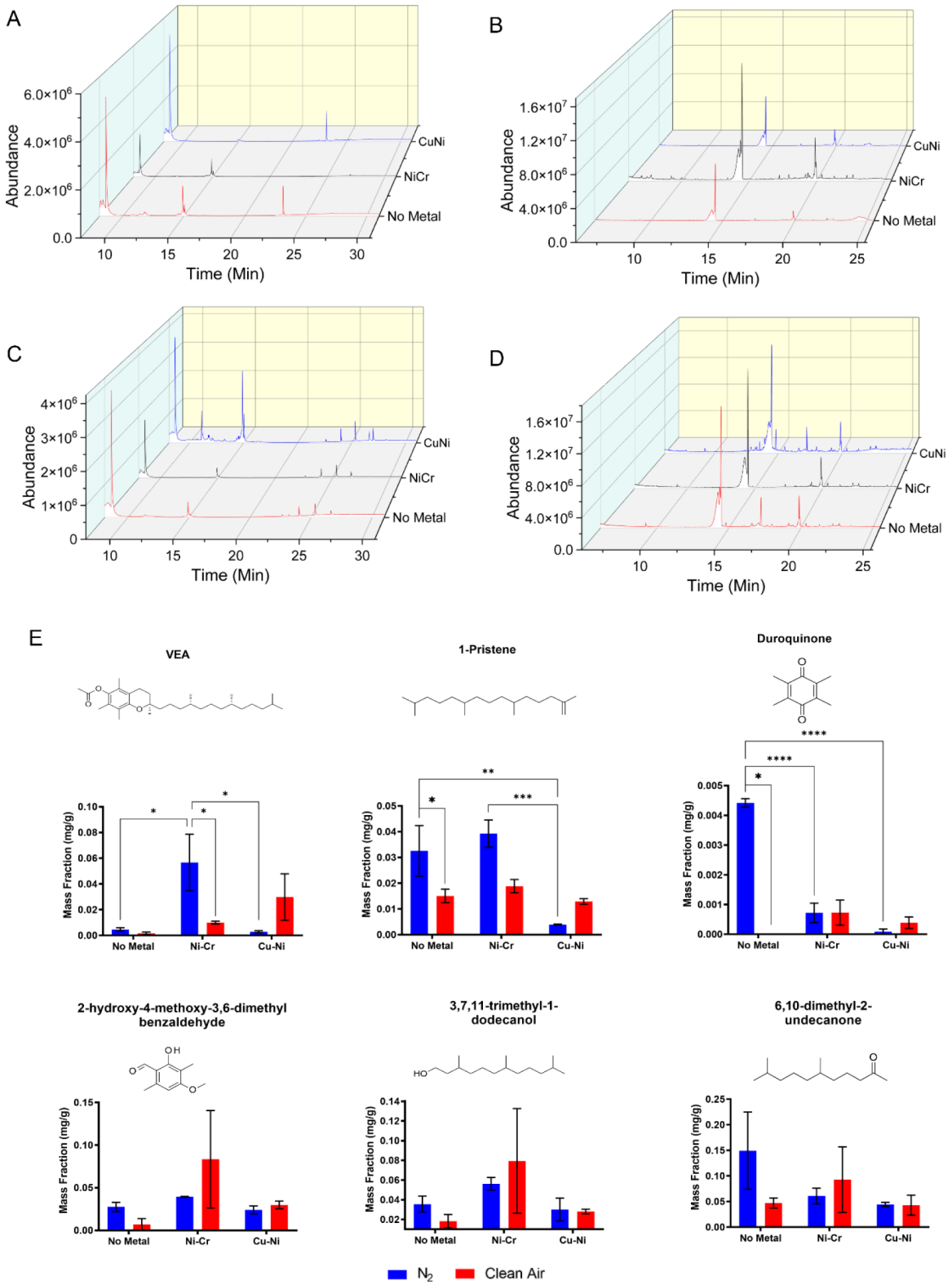

Figure 4. VEA product distribution under six different environmental conditions at 176 °C. Total ion chromatograms (TICs) were obtained from VEA pyrolysis in (A) N_2 environments in a nonpolar separation column, (B) N_2 in a polar separation column, (C) clean air in a nonpolar separation column, and (D) clean air in a polar separation column. (E) Masses of thermal degradation products, including VEA, 1-pristene, DQ, 2-hydroxy-4-methoxy-3,6-dimethyl benzaldehyde, 3,7,11-trimethyl-1-dodecanol, and 6,10-dimethyl-2-undecanone, formed under N_2 and clean air atmospheres at 176 °C. Results are expressed as means ± SEM (n = 3). One asterisk indicates $p < 0.05$. Two asterisks indicate $p < 0.01$.

oxidizing atmosphere and in the presence of Cu−Ni nanopowder. Significantly greater DQ masses could be seen in the inert environments in the presence of Cu−Ni nanopowder, while 2-hydroxy-4-methoxy-3,6-dimethyl benzaldehyde and 6,10-dimethyl-2-undecanone demonstrated greater masses in the presence of O_2 and Cu−Ni.

https://doi.org/10.1021/acs.chemrestox.2c00298
Chem. Res. Toxicol. 2023, 36, 83−93

3.3.2. Low-Temperature Experiments at 176 °C. Mass consumption at 176 °C showed a trend similar to that seen at 356 °C, with the addition of Cu−Ni nanopowder in either atmosphere resulting in a slight increase in mass consumed compared to the other environments (Figure S2B). The TIC obtained from heating VEA under each condition at 176 °C also shows a similar pattern, as while the addition of metal nanopowders did not appear to substantially shift the product distribution in an inert atmosphere (Figure 4A,B), the presence of Cu−Ni nanopowder resulted in the greatest number and abundance of peaks in an oxidizing atmosphere (Figure 4C,D), indicating substantial degradation of VEA similar to that seen in low-temperature vaping of VEA.[7] The appearance of the remaining VEA oil after heating to 176 °C, on the contrary, did not visibly differ between any of the environmental conditions (Figure S4).

However, there were notable differences in the normalized masses of each compound, VEA [t_R = 27.02 min (Figure 4A,C)], 1-pristene [t_R = 19.90 min (Figure 4B,D)], DQ [t_R = 16.52 min (Figure 4B,D)], 2-hydroxy-4-methoxy-3,6-dimethyl benzaldehyde [t_R = 22.67 min (Figure 4B,D)], 3,7,11-trimethyl-1-dodecanol [t_R = 19.20 min (Figure 4B,D)], and 6,10-dimethyl-2-undecanone [t_R = 17.23 min (Figure 4B,D)], at 176 °C compared to 356 °C shown in Figure 4E. Addition of Ni−Cr in the inert atmosphere resulted in significantly greater volatilization of VEA compared to that in the absence of metals; addition of Cu−Ni, however, resulted in greater mass of VEA in the oxidizing atmosphere than in the inert atmosphere, likely indicating greater volatilization of VEA in the presence of O_2 and Cu−Ni, and Ni−Cr in the absence of O_2. Likewise, there was no significant difference in the masses of 2-hydroxy-4-methoxy-3,6-dimethyl benzaldehyde, 3,7,11-trimethyl-1-dodecanol, and 6,10-dimethyl-2-undecanone.

The absence of metals and the presence of Ni−Cr alloy nanopowder in the inert atmosphere resulted in a significant increase in the mass of 1-pristene recovered compared to that in the presence of Cu−Ni; the presence of Cu−Ni in the inert atmosphere resulted in the smallest recovered mass of 1-pristene. There was no statistically significant difference in the oxidizing atmosphere between any treatments. An increase in the mass of 1-pristene in the presence of O_2 and Cu−Ni, compared to N_2 and Cu−Ni, was observed, though the increase was not significant. The masses of DQ recovered showed a trend similar to that of 1-pristene; here, the greatest mass was observed in the inert atmosphere in the absence of metals, with the addition of Ni−Cr and Cu−Ni greatly reducing the mass recovered. In the oxidizing atmosphere, the addition of Ni−Cr or Cu−Ni to the oxidizing atmosphere resulted in a nonsignificant increase in the mass of DQ when compared to the absence of metals, and a slightly greater mass when O_2 and Cu−Ni were present compared to that with N_2 and Cu−Ni.

3.3.3. Enhanced VEA Thermal Degradation in the Presence of Oxygen and Metals. Overall, the environment in which VEA was heated was observed to have a significant effect on the mass of the chosen compounds. The presence of Cu−Ni, especially in the oxidizing atmosphere, resulted in greater mass consumption and a greater number and abundance of thermal degradation products. Though VEA has been demonstrated to be thermally stable through pyrolysis pathways until higher temperatures are reached,[37] heating in the presence of Cu−Ni and O_2 resulted in substantial degradation of VEA into highly oxygenated products often observed in VEA vaping emissions. In contrast, the addition of Ni−Cr in the oxidizing atmosphere appeared to decrease the number and abundance of VEA degradation products, which concurs with observations made by Saliba et al.,[18] who found fresh nichrome wire to be the least reactive of e-cigarette coil types. These results may indicate the enhancement of oxidation pathways by O_2 in the atmosphere and transition metals in the body of the e-cigarette device and provide evidence for the importance of oxidation pathways and metal catalysis in low-temperature vaping.

Enhanced thermal degradation of organic compounds in the presence of metal catalysts has been documented in the literature. Catalysts may improve degradation by reducing the activation energy required for various thermal degradation pathways, including oxidation pathways. The activation energy required for pyrolysis of biosolids in wastewater treatment has been found to be significantly reduced in the presence of minerals or metal oxides acting as catalysts, reducing the temperature required to observe mass loss and degradation.[40,41] Moreover, upon investigation of the pyrolysis of biomass for the formation of biofuels, studies have found that the presence of transition metal catalysts allows for thermal degradation of organic compounds at lower pyrolysis temperatures, accelerates pyrolysis, and influences the pyrolysis product distribution.[30,42,43] More specifically, Hubble et al.[30] also demonstrated that Cu and Ni are more catalytically efficient than other investigated metal oxides in the pyrolysis of biomass for the formation of biofuels.[30] The presence of Cu in particular demonstrated the ability to catalyze devolatilization of biomass at lower pyrolysis temperatures than commonly reported. It is highly likely that these phenomena can occur in various organic systems other than biosolids or biochar, including the pyrolysis of e-liquids. In essence, these results clearly indicate the potential role of oxidation by O_2 and metal catalysis as important factors to consider when attempting to understand the pathways and required temperatures for e-liquid thermal degradation.

3.4. Generation of OH Radicals. In addition to organic oxidants and metal particles, several studies have indicated the potential for vaping to generate various reactive oxygen species (ROS), including superoxide ($O_2^{\bullet-}$) and OH radicals.[4,21,26,44] Recent studies by Son et al.[45] and Zhao et al.[25] have directly measured the formation of OH radicals in vaping emissions; these radicals may not only interact with biological systems to induce oxidative damage but also induce further oxidation of e-liquids and thermal degradation products, resulting in the formation of highly oxygenated compounds with great oxidative potential.[46]

A few potential sources of OH radicals in e-cigarette systems have been suggested, including through the oxidation of organic e-liquids by O_2 and transition metal redox reactions (such as the Fenton and Fenton-like reactions).[38,45,47,48] To investigate whether enhancement of VEA degradation in the presence of O_2 and Cu−Ni could be attributed to the increased OH production, VEA was heated at 176 °C in N_2 and clean air atmospheres in the presence and absence of Cu−Ni alloy nanopowder, and OH radical formation was directly measured using the TPT assay. In the absence of Cu−Ni alloy nanopowder, the production of OH was significantly increased when VEA was heated in an oxidizing atmosphere compared to an inert atmosphere (Figure 5). When Cu−Ni was added, the production of OH was significantly enhanced in an oxidizing atmosphere, but the addition of Cu−Ni in the inert

https://doi.org/10.1021/acs.chemrestox.2c00298
Chem. Res. Toxicol. 2023, 36, 83−93

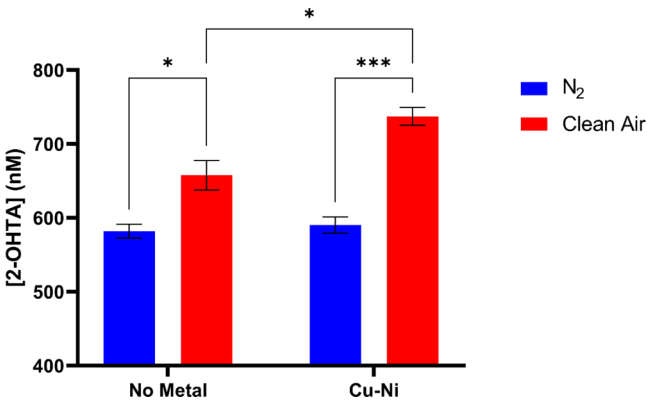

Figure 5. 2-OHTA generated by VEA heated in inert (N_2) and oxidizing (clean air) atmospheres in the absence and presence of Cu−Ni alloy nanopowder. Results are expressed as means ± SEM (n = 3). One asterisk indicates $p < 0.05$. Three asterisks indicate $p < 0.001$.

atmosphere resulted in no significant difference. These results indicate that atmospheric O_2 is a source of OH formation and that at low temperatures, Cu−Ni may enhance OH formation in the presence of O_2 via catalytic reactions. These findings are consistent with our GC/MS analysis, highlighting the importance of O_2 and oxidation reactions in VEA degradation, as well as the role of metals in catalyzing the reactions.

Prior research has shown that transition metals, particularly metals such as Fe and Cu, may catalyze the activation of O_2 to form OH radicals.[49] This O_2-dependent OH radical formation pathway may explain why OH radicals are enhanced only in the oxidizing atmosphere, not in the presence of Cu−Ni in the inert atmosphere. However, the presence of OH radicals in the inert atmosphere does suggest a secondary source of OH radicals, potentially from heating of VEA alone, reaction of degradation products in the aqueous media used to trap radicals, or intrusion into the instrument from the lab atmosphere.

Regardless, the presence and enhanced formation of OH radicals are noteworthy as a recent study by Li et al.[38] suggested that many degradation products of VEA may result from OH radical- and O_2-mediated reactions. Radicals such as OH may initiate bond homolysis, dehydration, or H-abstraction on the side chain of VEA, followed by RO_2 radical-mediated chemistry to form highly oxygenated products observed in vaping emissions.[38,50] Such degradation pathways may occur simultaneously through pyrolysis-induced degradation, producing unique compounds that cannot be explained through pyrolysis alone. In our results, the enhanced formation of OH radicals in an oxidizing environment and the increased number of degradation products observed in the presence of O_2 and Cu−Ni provide further evidence of oxidative pathways as a dominant factor in VEA degradation, particularly at low temperatures. Furthermore, the catalytic effect of metals from heating coils in the presence of O_2 at low temperatures may explain the abundance of low-temperature thermal degradation products in vaping scenarios that are not explained through pyrolysis alone.[7]

3.5. Potential Limitations. While this study improves our understanding of the catalytic effect of metals when vaping, some limitations must be noted when these results are applied to real-world vaping scenarios. First, this study investigates the influence of three metals commonly found in high abundance in the body of e-cigarette coils and cartridges.[12] It should be noted that real-life devices may contain a mixture of various metal alloys and several metals not investigated here, such as Mn, Zn, Sn, etc.[12,13] Large amounts of other redox-active transition metals, such as Fe, may further alter the chemical composition of resulting e-cigarette emissions through alternative metal−organic interactions or enhanced production of OH radicals. While this study chose to investigate metals that were representative of common e-cigarette devices, more studies are needed to fully characterize the influence of various metals on the chemical composition of e-cigarette emissions. Additionally, the limitations of the cold trap method have been previously described.[4,7] This method was optimized for the detection of compounds with boiling points at or above the temperature of dry ice without the use of additional derivatization techniques. As a result, while this method is effective for capturing compounds such as VEA and DQ, highly volatile and reactive compounds like ketene and various carbonyls may be produced from VEA degradation but are not detectable. Nonetheless, we do not expect that the inability to detect certain reactive or highly volatile compounds will have a significant impact on the interpretation of our findings.

4. CONCLUSION AND IMPLICATIONS

This study examines the effects of O_2 and two metal alloy nanopowders on the chemical composition of e-cigarette emissions. Our results show significant degradation of VEA at high and low temperatures in the presence of O_2 and Cu−Ni alloy nanopowder. Moreover, VEA heated in clean air resulted in significantly greater OH production than in inert atmospheres, with Cu−Ni metal alloy enhancing OH production only in the presence of O_2. Ultimately, these results highlight the importance of oxidation pathways in the low-temperature degradation of e-liquids catalyzed by metals. The production of many oxygenated VEA and other e-liquid vaping products likely cannot be explained by the pyrolysis of VEA alone; rather, it is likely that multiple, simultaneous pathways degrade the parent oils. As such, the role of O_2 and oxidation pathways must be considered when predicting e-liquid thermal degradation.

Furthermore, the observed presence of OH radicals in VEA emissions not only provides evidence of the role of oxidation in the low-temperature degradation of VEA but also has important implications for the health of vape users. First, as evidenced here, the promotion of OH radical formation likely promotes oxidation and the formation of oxygenated degradation products. Exposure to such products through vaping may result in oxidative damage to biomolecules;[51−54] consideration of OH radical-mediated pathways may assist in predictive models attempting to characterize potential degradation products that may cause harm to users. Second, inhalation of OH radicals alone may pose a serious risk of oxidative damage. OH radicals are considered one of the most strongly oxidizing ROS species.[55,56] These radicals have immense potential to interact with biomolecules such as proteins and lipids in lung lining fluid[56−58] and have been found to induce DNA strand breaks and the formation of oxidative DNA adducts.[59,60] To fully understand the risk of oxidative damage associated with vaping, it is clearly critical to consider the formation of OH radical species and OH-mediated reactions.

Overall, the findings of this study provide insight into the potential role of O_2 and metals in not only e-liquid degradation but also various other systems investigating the inhalation risk

https://doi.org/10.1021/acs.chemrestox.2c00298
Chem. Res. Toxicol. 2023, 36, 83−93

of organic compounds heated in the presence of O_2 or metals. These results emphasize that the consideration of many factors is crucial for future exposure and risk assessment. Future studies should focus on the impact of these oxidation pathways and how they interact with other varying parameters (such as puffing topography, temperature, and design of e-cigarette devices) to influence the chemical composition of vaping emissions.

■ ASSOCIATED CONTENT

Supporting Information

The Supporting Information is available free of charge at https://pubs.acs.org/doi/10.1021/acs.chemrestox.2c00298.

Summary of the percent mass values of VEA remaining in crucibles at set temperatures (Table S1), calibration curve of 2-OHTA (Figure S1), mass of VEA consumed during tube furnace reactions (Figure S2), images of crucibles taken after they had been heated at 356 °C (Figure S3), and images of crucibles taken after they had been heated at 176 °C (Figure S4) (PDF)

■ AUTHOR INFORMATION

Corresponding Author

Ying-Hsuan Lin − *Environmental Toxicology Graduate Program, University of California, Riverside, California 92521, United States; Department of Environmental Sciences, University of California, Riverside, California 92521, United States;* orcid.org/0000-0001-8904-1287; Email: ying-hsuan.lin@ucr.edu

Authors

Alexa Canchola − *Environmental Toxicology Graduate Program, University of California, Riverside, California 92521, United States;* orcid.org/0000-0001-8285-4795

Siri Langmo − *Department of Evolution, Ecology, and Organismal Biology, University of California, Riverside, California 92521, United States*

Ruth Meletz − *Department of Environmental Sciences, University of California, Riverside, California 92521, United States;* orcid.org/0000-0003-1038-248X

Michael Lum − *Department of Environmental Sciences, University of California, Riverside, California 92521, United States*

Complete contact information is available at: https://pubs.acs.org/10.1021/acs.chemrestox.2c00298

Author Contributions

CRediT: **Alexa Canchola** conceptualization, formal analysis, investigation, methodology, visualization, writing-original draft, writing-review & editing; **Siri Langmo** formal analysis, investigation, writing-original draft; **Ruth Meletz** investigation, writing-review & editing; **Michael Lum** investigation, writing-review & editing; **Ying-Hsuan Lin** conceptualization, funding acquisition, investigation, methodology, project administration, supervision, writing-original draft, writing-review & editing.

Notes

The authors declare no competing financial interest.

■ ACKNOWLEDGMENTS

Y.-H.L. gratefully acknowledges support from the the University of California Riverside (UCR) Regents' Faculty Development Award and the University of California Tobacco-Related Disease Research Program (T32IP5141) for this research. A.C. was supported by an NRSA T32 training grant (T32ES18827). R.M. was supported by a grant from the National Institutes of Health (T34GM062756). S.L. was supported by the UCR Chancellor's Research Fellowship Award. The authors gratefully acknowledge the UCR Materials Science and Engineering Facilities for the use of their instrumentation.

■ ABBREVIATIONS

VEA, vitamin E acetate; DQ, duroquinone; ROS, reactive oxygen species; Ni−Cr, nickel−chromium; Cu−Ni, copper−nickel

■ REFERENCES

(1) Centers for Disease Control and Prevention. Outbreak of Lung Injury Associated with the Use of E-Cigarette, or Vaping, Products. https://www.cdc.gov/tobacco/basic_information/e-cigarettes/severe-lung-disease.html.

(2) Braymiller, J. L.; Barrington-Trimis, J. L.; Leventhal, A. M.; Islam, T.; Kechter, A.; Krueger, E. A.; Cho, J.; Lanza, I.; Unger, J. B.; McConnell, R. Assessment of Nicotine and Cannabis Vaping and Respiratory Symptoms in Young Adults. *JAMA Network Open* **2020**, *3* (12), No. e2030189.

(3) Jiang, H.; Ahmed, C. M. S.; Martin, T. J.; Canchola, A.; Oswald, I. W. H.; Garcia, J. A.; Chen, J. Y.; Koby, K. A.; Buchanan, A. J.; Zhao, Z.; Zhang, H.; Chen, K.; Lin, Y.-H. Chemical and Toxicological Characterization of Vaping Emission Products from Commonly Used Vape Juice Diluents. *Chem. Res. Toxicol.* **2020**, *33* (8), 2157−2163.

(4) Canchola, A.; Ahmed, C. M. S.; Chen, K.; Chen, J. Y.; Lin, Y.-H. Formation of Redox-Active Duroquinone from Vaping of Vitamin E Acetate Contributes to Oxidative Lung Injury. *Chem. Res. Toxicol.* **2022**, *35* (2), 254−264.

(5) Chen, J. Y.; Canchola, A.; Lin, Y.-H. Carbonyl Composition and Electrophilicity in Vaping Emissions of Flavored and Unflavored E-Liquids. *Toxics* **2021**, *9* (12), 345.

(6) Bekki, K.; Uchiyama, S.; Ohta, K.; Inaba, Y.; Nakagome, H.; Kunugita, N. Carbonyl Compounds Generated from Electronic Cigarettes. *International Journal of Environmental Research and Public Health* **2014**, *11* (11), 11192−11200.

(7) Canchola, A.; Meletz, R.; Khandakar, R. A.; Woods, M.; Lin, Y.-H. Temperature dependence of emission product distribution from vaping of vitamin E acetate. *PLoS One* **2022**, *17* (3), No. e0265365.

(8) Lynch, J.; Lorenz, L.; Brueggemeyer, J. L.; Lanzarotta, A.; Falconer, T. M.; Wilson, R. A. Simultaneous Temperature Measurements and Aerosol Collection During Vaping for the Analysis of Δ9-Tetrahydrocannabinol and Vitamin E Acetate Mixtures in Ceramic Coil Style Cartridges. *Front. Chem.* **2021**, *9*, 643.

(9) Wu, D.; O'Shea, D. F. Potential for release of pulmonary toxic ketene from vaping pyrolysis of vitamin E acetate. *Proc. Natl. Acad. Sci. U.S.A.* **2020**, *117* (12), 6349−6355.

(10) Kovach, A. L.; Carter, R. R.; Thornburg, J. W.; Wiethe, R.; Fennell, T. R.; Wiley, J. L. Thermal Degradants Identified from the Vaping of Vitamin E Acetate. *Journal of Analytical Toxicology* **2022**, *46* (7), 750−756.

(11) Matsumoto, S.; Traber, M. G.; Leonard, S. W.; Choi, J.; Fang, X.; Maishan, M.; Wick, K. D.; Jones, K. D.; Calfee, C. S.; Gotts, J. E.; Matthay, M. A. Aerosolized vitamin E acetate causes oxidative injury in mice and in alveolar macrophages. *Am. J. Physiol.* **2022**, *322* (6), L771−L783.

(12) McDaniel, C.; Mallampati, S. R.; Wise, A. Metals in Cannabis Vaporizer Aerosols: Sources, Possible Mechanisms, and Exposure Profiles. *Chem. Res. Toxicol.* **2021**, *34* (11), 2331−2342.

(13) Omaiye, E. E.; Williams, M.; Bozhilov, K. N.; Talbot, P. Design features and elemental/metal analysis of the atomizers in pod-style electronic cigarettes. *PLoS One* **2021**, *16* (3), No. e0248127.

(14) Gonzalez-Jimenez, N.; Gray, N.; Pappas, R. S.; Halstead, M.; Lewis, E.; Valentin-Blasini, L.; Watson, C.; Blount, B. Analysis of Toxic Metals in Aerosols from Devices Associated with Electronic Cigarette, or Vaping, Product Use Associated Lung Injury. *Toxics* **2021**, *9* (10), 240.
(15) Gray, N.; Halstead, M.; Gonzalez-Jimenez, N.; Valentin-Blasini, L.; Watson, C.; Pappas, R. S. Analysis of Toxic Metals in Liquid from Electronic Cigarettes. *International Journal of Environmental Research and Public Health* **2019**, *16* (22), 4450.
(16) Williams, M.; Villarreal, A.; Bozhilov, K.; Lin, S.; Talbot, P. Metal and Silicate Particles Including Nanoparticles Are Present in Electronic Cigarette Cartomizer Fluid and Aerosol. *PLoS One* **2013**, *8* (3), No. e57987.
(17) Chun, L. F.; Moazed, F.; Calfee, C. S.; Matthay, M. A.; Gotts, J. E. Pulmonary toxicity of e-cigarettes. *American Journal of Physiology-Lung Cellular and Molecular Physiology* **2017**, *313* (2), L193−L206.
(18) Saliba, N. A.; El Hellani, A.; Honein, E.; Salman, R.; Talih, S.; Zeaiter, J.; Shihadeh, A. Surface chemistry of electronic cigarette electrical heating coils: Effects of metal type on propylene glycol thermal decomposition. *Journal of Analytical and Applied Pyrolysis* **2018**, *134*, 520−525.
(19) Jensen, R. P.; Strongin, R. M.; Peyton, D. H. Solvent chemistry in the electronic cigarette reaction vessel. *Sci. Rep.* **2017**, *7* (1), 42549.
(20) Behar, R. Z.; Hua, M.; Talbot, P. Puffing Topography and Nicotine Intake of Electronic Cigarette Users. *PLoS One* **2015**, *10* (2), No. e0117222.
(21) Zhao, T.; Shu, S.; Guo, Q.; Zhu, Y. Effects of design parameters and puff topography on heating coil temperature and mainstream aerosols in electronic cigarettes. *Atmos. Environ.* **2016**, *134*, 61−69.
(22) Li, Y.; Burns, A. E.; Tran, L. N.; Abellar, K. A.; Poindexter, M.; Li, X.; Madl, A. K.; Pinkerton, K. E.; Nguyen, T. B. Impact of e-Liquid Composition, Coil Temperature, and Puff Topography on the Aerosol Chemistry of Electronic Cigarettes. *Chem. Res. Toxicol.* **2021**, *34* (6), 1640−1654.
(23) Lechasseur, A.; Altmejd, S.; Turgeon, N.; Buonanno, G.; Morawska, L.; Brunet, D.; Duchaine, C.; Morissette, M. C. Variations in coil temperature/power and e-liquid constituents change size and lung deposition of particles emitted by an electronic cigarette. *Physiological reports* **2019**, *7* (10), No. e14093.
(24) Zhao, D.; Navas-Acien, A.; Ilievski, V.; Slavkovich, V.; Olmedo, P.; Adria-Mora, B.; Domingo-Relloso, A.; Aherrera, A.; Kleiman, N. J.; Rule, A. M.; Hilpert, M. Metal concentrations in electronic cigarette aerosol: Effect of open-system and closed-system devices and power settings. *Environmental Research* **2019**, *174*, 125−134.
(25) Zhao, J.; Zhang, Y.; Sisler, J. D.; Shaffer, J.; Leonard, S. S.; Morris, A. M.; Qian, Y.; Bello, D.; Demokritou, P. Assessment of reactive oxygen species generated by electronic cigarettes using acellular and cellular approaches. *Journal of Hazardous Materials* **2018**, *344*, 549−557.
(26) Cirillo, S.; Urena, J. F.; Lambert, J. D.; Vivarelli, F.; Canistro, D.; Paolini, M.; Cardenia, V.; Rodriguez-Estrada, M. T.; Richie, J. P.; Elias, R. J. Impact of electronic cigarette heating coil resistance on the production of reactive carbonyls, reactive oxygen species and induction of cytotoxicity in human lung cancer cells in vitro. *Regul. Toxicol. Pharmacol.* **2019**, *109*, 104500.
(27) Bitzer, Z. T.; Goel, R.; Reilly, S. M.; Foulds, J.; Muscat, J.; Elias, R. J.; Richie, J. P. Effects of Solvent and Temperature on Free Radical Formation in Electronic Cigarette Aerosols. *Chem. Res. Toxicol.* **2018**, *31* (1), 4−12.
(28) Geiss, O.; Bianchi, I.; Barrero-Moreno, J. Correlation of volatile carbonyl yields emitted by e-cigarettes with the temperature of the heating coil and the perceived sensorial quality of the generated vapours. *International Journal of Hygiene and Environmental Health* **2016**, *219* (3), 268−277.
(29) Ushikusa, T.; Maruyama, T.; Niiya, I. Pyrolysis behavior and thermostability of tocopherols. *Nihon Yukagakkaishi* **1991**, *40* (12), 1073−1079.
(30) Hubble, A. H.; Ryan, E. M.; Goldfarb, J. L. Enhancing pyrolysis gas and bio-oil formation through transition metals as in situ catalysts. *Fuel* **2022**, *308*, 121900.
(31) Jaegers, N. R.; Hu, W.; Weber, T. J.; Hu, J. Z. Low-temperature (< 200 °C) degradation of electronic nicotine delivery system liquids generates toxic aldehydes. *Sci. Rep.* **2021**, *11* (1), 7800.
(32) Zhu, J.; Niu, J.; Das, D.; Cabecinha, A.; Abramovici, H. In-situ TD-GCMS measurements of oxidative products of monoterpenes at typical vaping temperatures: implications for inhalation exposure to vaping products. *Sci. Rep.* **2022**, *12* (1), 11019.
(33) D3452-06, A Standard Practice for Rubber Identification by Pyrolysis-Gas Chromatography. 2012.
(34) Barreto, J. C.; Smith, G. S.; Strobel, N. H. P.; McQuillin, P. A.; Miller, T. A. Terephthalic acid: A dosimeter for the detection of hydroxyl radicals in vitro. *Life Sciences* **1994**, *56* (4), PL89−PL96.
(35) Linxiang, L.; Abe, Y.; Nagasawa, Y.; Kudo, R.; Usui, N.; Imai, K.; Mashino, T.; Mochizuki, M.; Miyata, N. An HPLC assay of hydroxyl radicals by the hydroxylation reaction of terephthalic acid. *Biomedical Chromatography* **2004**, *18* (7), 470−474.
(36) Saran, M.; Summer, K. H. Assaying for hydroxyl radicals: Hydroxylated terephthalate is a superior fluorescence marker than hydroxylated benzoate. *Free Radical Research* **1999**, *31* (5), 429−436.
(37) EFSA Panel on Food Contact Materials, Enzymes, Flavourings and Processing Aids (CEF).. Safety assessment of the substance α-tocopherol acetate for use in food contact materials. *EFSA J.* **2016**, *14* (3), 4412.
(38) Li, Y.; Dai, J.; Tran, L. N.; Pinkerton, K. E.; Spindel, E. R.; Nguyen, T. B. Vaping Aerosols from Vitamin E Acetate and Tetrahydrocannabinol Oil: Chemistry and Composition. *Chem. Res. Toxicol.* **2022**, *35* (6), 1095−1109.
(39) Mikheev, V. B.; Klupinski, T. P.; Ivanov, A.; Lucas, E. A.; Strozier, E. D.; Fix, C. Particle size distribution and chemical composition of aerosolized vitamin E acetate. *Aerosol Sci. Technol.* **2020**, *54* (9), 993−998.
(40) Patel, S.; Kundu, S.; Halder, P.; Rickards, L.; Paz-Ferreiro, J.; Surapaneni, A.; Madapusi, S.; Shah, K. Thermogravimetric Analysis of biosolids pyrolysis in the presence of mineral oxides. *Renewable Energy* **2019**, *141*, 707−716.
(41) Shao, J.; Yan, R.; Chen, H.; Yang, H.; Lee, D. H. Catalytic effect of metal oxides on pyrolysis of sewage sludge. *Fuel Process. Technol.* **2010**, *91* (9), 1113−1118.
(42) Su, G.; Ong, H. C.; Mofijur, M.; Mahlia, T. M. I.; Ok, Y. S. Pyrolysis of waste oils for the production of biofuels: A critical review. *Journal of Hazardous Materials* **2022**, *424*, 127396.
(43) Hakeem, I. G.; Halder, P.; Dike, C. C.; Chiang, K.; Sharma, A.; Paz-Ferreiro, J.; Shah, K. Advances in biosolids pyrolysis: Roles of pre-treatments, catalysts, and co-feeding on products distribution and high-value chemical production. *Journal of Analytical and Applied Pyrolysis* **2022**, *166*, 105608.
(44) Goel, R.; Durand, E.; Trushin, N.; Prokopczyk, B.; Foulds, J.; Elias, R. J.; Richie, J. P. Highly Reactive Free Radicals in Electronic Cigarette Aerosols. *Chem. Res. Toxicol.* **2015**, *28* (9), 1675−1677.
(45) Son, Y.; Mishin, V.; Laskin, J. D.; Mainelis, G.; Wackowski, O. A.; Delnevo, C.; Schwander, S.; Khlystov, A.; Samburova, V.; Meng, Q. Hydroxyl Radicals in E-Cigarette Vapor and E-Vapor Oxidative Potentials under Different Vaping Patterns. *Chem. Res. Toxicol.* **2019**, *32* (6), 1087−1095.
(46) Halliwell, B.; Gutteridge, J. M. C. *Free radicals in biology and medicine*; Oxford University Press: New York, 2015.
(47) Valavanidis, A.; Fiotakis, K.; Bakeas, E.; Vlahogianni, T. Electron paramagnetic resonance study of the generation of reactive oxygen species catalysed by transition metals and quinoid redox cycling by inhalable ambient particulate matter. *Redox Report* **2005**, *10* (1), 37−51.
(48) Laino, T.; Tuma, C.; Moor, P.; Martin, E.; Stolz, S.; Curioni, A. Mechanisms of Propylene Glycol and Triacetin Pyrolysis. *J. Phys. Chem. A* **2012**, *116* (18), 4602−4609.
(49) Cai, J.; Li, H.; Feng, K.; Cheng, Y.; He, S.; Takaoka, M. Low-temperature degradation of humic acid via titanium zirconium

oxide@copper single-atom activating oxygen: Mechanism and pathways. *Chemical Engineering Journal* **2022**, *450*, 138239.
(50) Houle, F. A.; Hinsberg, W. D.; Wilson, K. R. Oxidation of a model alkane aerosol by OH radical: the emergent nature of reactive uptake. *Phys. Chem. Chem. Phys.* **2015**, *17* (6), 4412−4423.
(51) Bonner, E.; Chang, Y.; Christie, E.; Colvin, V.; Cunningham, B.; Elson, D.; Ghetu, C.; Huizenga, J.; Hutton, S. J.; Kolluri, S. K.; Maggio, S.; Moran, I.; Parker, B.; Rericha, Y.; Rivera, B. N.; Samon, S.; Schwichtenberg, T.; Shankar, P.; Simonich, M. T.; Wilson, L. B.; Tanguay, R. L. The chemistry and toxicology of vaping. *Pharmacology & Therapeutics* **2021**, *225*, 107837.
(52) Sundar, I. K.; Javed, F.; Romanos, G. E.; Rahman, I. E-cigarettes and flavorings induce inflammatory and pro-senescence responses in oral epithelial cells and periodontal fibroblasts. *Oncotarget* **2016**, *7* (47), 77196.
(53) Cheng, G.; Guo, J.; Carmella, S. G.; Lindgren, B.; Ikuemonisan, J.; Niesen, B.; Jensen, J.; Hatsukami, D. K.; Balbo, S.; Hecht, S. S. Increased acrolein-DNA adducts in buccal brushings of e-cigarette users. *Carcinogenesis* **2022**, *43* (5), 437−444.
(54) Paiano, V.; Maertens, L.; Guidolin, V.; Yang, J.; Balbo, S.; Hecht, S. S. Quantitative Liquid Chromatography-Nanoelectrospray Ionization-High-Resolution Tandem Mass Spectrometry Analysis of Acrolein-DNA Adducts and Etheno-DNA Adducts in Oral Cells from Cigarette Smokers and Nonsmokers. *Chem. Res. Toxicol.* **2020**, *33* (8), 2197−2207.
(55) Valavanidis, A.; Salika, A.; Theodoropoulou, A. Generation of hydroxyl radicals by urban suspended particulate air matter. The role of iron ions. *Atmos. Environ.* **2000**, *34* (15), 2379−2386.
(56) Marusawa, H.; Ichikawa, K.; Narita, N.; Murakami, H.; Ito, K.; Tezuka, T. Hydroxyl radical as a strong electrophilic species. *Bioorganic & medicinal chemistry* **2002**, *10* (7), 2283−2290.
(57) Riley, P. A. Free radicals in biology: oxidative stress and the effects of ionizing radiation. *International journal of radiation biology* **1994**, *65* (1), 27−33.
(58) Therond, P. *Oxidative stress and damages to biomolecules (lipids, proteins, DNA)* **2006**, *64*, 383−389.
(59) Leanderson, P.; Tagesson, C. Cigarette smoke-induced DNA damage in cultured human lung cells: role of hydroxyl radicals and endonuclease activation. *Chemico-biological interactions* **1992**, *81* (1−2), 197−208.
(60) Chatgilialoglu, C.; Ferreri, C.; Krokidis, M. G.; Masi, A.; Terzidis, M. A. On the relevance of hydroxyl radical to purine DNA damage. *Free Radical Research* **2021**, *55* (4), 384−404.

https://doi.org/10.1021/acs.chemrestox.2c00298
Chem. Res. Toxicol. 2023, 36, 83−93